

Experimental Study of the $\text{Bi}_2\text{O}_3\text{-Fe}_2\text{O}_3$ Pseudo-Binary System

A. Maître, M. François, and J.C. Gachon

(Submitted 2 June 2003; in revised form 15 August 2003)

As part of a general contribution to the study of accelerator driven system (ADS) nuclear reactor feasibility, a study of the five-component system Bi-Fe-Hg-O-Pb was undertaken. New results about the quasi-binary $\text{Bi}_2\text{O}_3\text{-Fe}_2\text{O}_3$ are presented in this paper. The phase diagram was reinvestigated by differential scanning calorimetry, x-ray diffraction, and electron probe microanalysis. A new compound was discovered and characterized: $\text{Bi}_{25}\text{FeO}_{40}$. Its crystallographic structure was refined. Invariant and transition temperatures are given, as well as phase compositions.

1. Introduction

Among the nuclear reactors for power generation of the future, accelerator driven systems (ADS) will use a proton accelerator, on the one hand, and a liquid metal target, on the other hand, to yield neutrons that will sustain the fission reaction in a subcritical core. The liquid will be the eutectic alloy Pb + 55.2 wt.% Bi. It will be both the fast neutron source (spallation reactions with the incident energetic protons) and a heat carrier [2000Kne].

To predict the long-term behavior of the structural material (T 91 steel, 9 Cr, 1 Mo), containing the liquid bath, thermodynamic knowledge of the five-component system Bi-Fe-Hg-O-Pb is needed:

- In the liquid proton target, spallation reactions may yield impurities [2002Vil] and especially non negligible quantities of mercury.
- On the surface of T 91 samples subjected to long term corrosion tests in conditions reproducing those of the reactor [2001Bar, 2001Faz, 2002Maï1], products like Fe_3O_4 , $\text{Fe}_{(1-x)}\text{Cr}_x\text{Fe}_2\text{O}_4$, $\text{Bi}_{25}\text{FeO}_{40}$, and PbO have been found.

The subsystem Pb-Bi-Hg has already been studied in the laboratory [2002Mai2], and a new compound with a stoichiometry around $\text{Bi}_7\text{Hg}_4\text{Pb}_9$ has been found. Its stability range is below 37 °C. A strong diminution of the liquidus temperatures is induced by small additions of mercury (<1 wt.%).

To continue the description of the ternary subsystems of Bi-Fe-Hg-O-Pb, we have undertaken the study of Bi-Fe-O. Very few papers dealing with this system are found in the literature. At first, the isopleth $\text{Bi}_2\text{O}_3\text{-Fe}_2\text{O}_3$, which includes several corrosion products of the T91 was characterized. Koizumi et al. [1964Koi] and Speranskaya et al. [1965Spe]

have published two contradictory versions (Fig. 1a and 1b); the main points being the intermediate compound near Bi_2O_3 , the invariants, and the allotropic transformation in BiFeO_3 . In more recent works concerning $\text{Bi}_2\text{O}_3\text{-Fe}_2\text{O}_3$, physico-chemical characteristics have been determined without questioning the phase equilibria [1989Dim, 1989Tan, 2000Luo, 2000Pas].

2. Experimental

The raw materials used were supplied by Riedel-de-Haën (St. Louis, MO) (Fe_2O_3 , 99.99 wt.%) and Alfa (Ward Hill, MA), (Bi_2O_3 , 99.99 wt.%). Their main characteristics are given in Table 1. Scanning electron microscopy (SEM) was used to determine the morphology of the powders (Fig. 2a and 2b).

Mixtures of oxides were prepared under air by weighing and mixing the components in an agate mortar before introducing them into platinum crucibles, which were then sealed by arc welding to limit weight losses, i.e., composition changes during heat treatments.

The first treatment of heating at 1 °C min⁻¹ up to 1000 °C, several hours at that temperature, and then cooling at 1 °C min⁻¹ ensured the reaction between the components. Then differential scanning calorimetry (DSC) from room temperature to 1000 °C with a calorimeter designed and built in the laboratory [1986Gac] gave the temperatures of transformation and the relative quantities of products in the samples. The temperature cycles were composed of heating and cooling at a rate of 2 °C min⁻¹ with an annealing of 15 min at the top temperature (Fig. 3a). After DSC experiments, the products were subjected to x-ray diffraction (Philips X'pert Pro, Eindhoven, The Netherlands, $\lambda = 0.154056$ nm), SEM (Hitachi S-2500, Tokyo, Japan), and electron probe microanalysis (EPMA; CAMECA SX100, Courbevoie, France). For EPMA, the instrument operating conditions were 10 kV accelerating voltage and 10 mA probe current, and the size of the excited zone was about 1 μm^3 . Accumulation times on standards and samples were determined to achieve good accuracy for the element content analyses. In addition, EPMA on samples heat-treated

A. Maître, M. François, and J.C. Gachon, Laboratoire de Chimie du Solide Minéral UMR CNRS 7555 – Université Henri Poincaré, Faculty of Science and Technology, B.P. 239 – F-54506, Vandoeuvre-les-Nancy, Cedex, France. Contact e-mail: Alexandre.Maitre@lcsm.uhp-nancy.fr.

Section I: Basic and Applied Research

Table 1 Main Characteristics of the Oxides

Oxide (manufacturer)	Purity, wt. %	Specific Mass, gcm ³	Specific Area BET, m ² g ⁻¹ min	Size (from Manufacturer, μm)	Size from BET, μm (a)
Bi ₂ O ₃ (Riedel-de-Haën)	99.99	8.90	4.7	1-5	0.14
Fe ₂ O ₃ (Alfa)	99.99	5.25	3.0	1-5	0.38

(a) The mean diameter of the grains is deduced from $d_m = 6 \times \rho / S_{BET}$ with S_{BET} the specific area determined by the BET method.

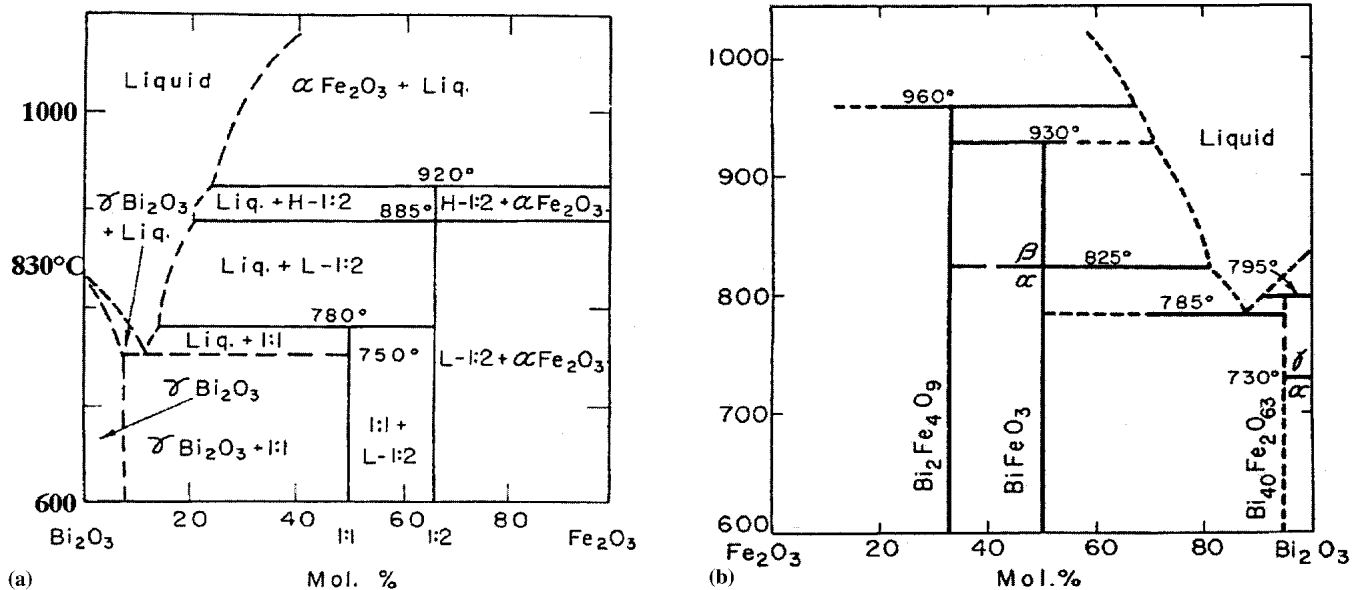


Fig. 1 Bi₂O₃-Fe₂O₃ phase diagrams as proposed by (a) [1964Koi] and (b) [1965Spe]

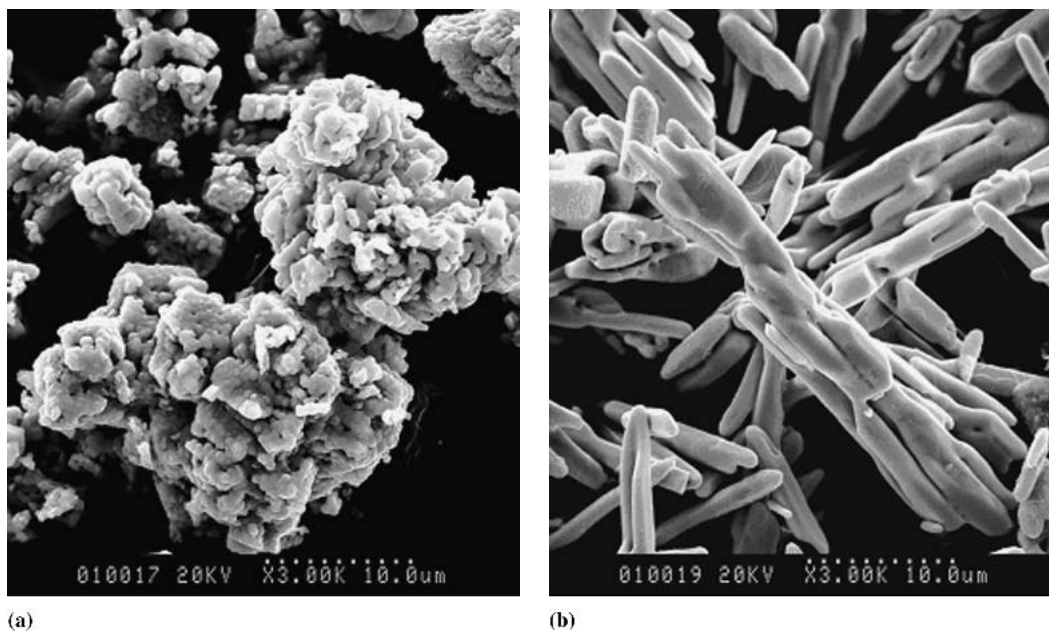


Fig. 2 SEM photomicrographs of (a) Fe₂O₃ and (b) Bi₂O₃ powders

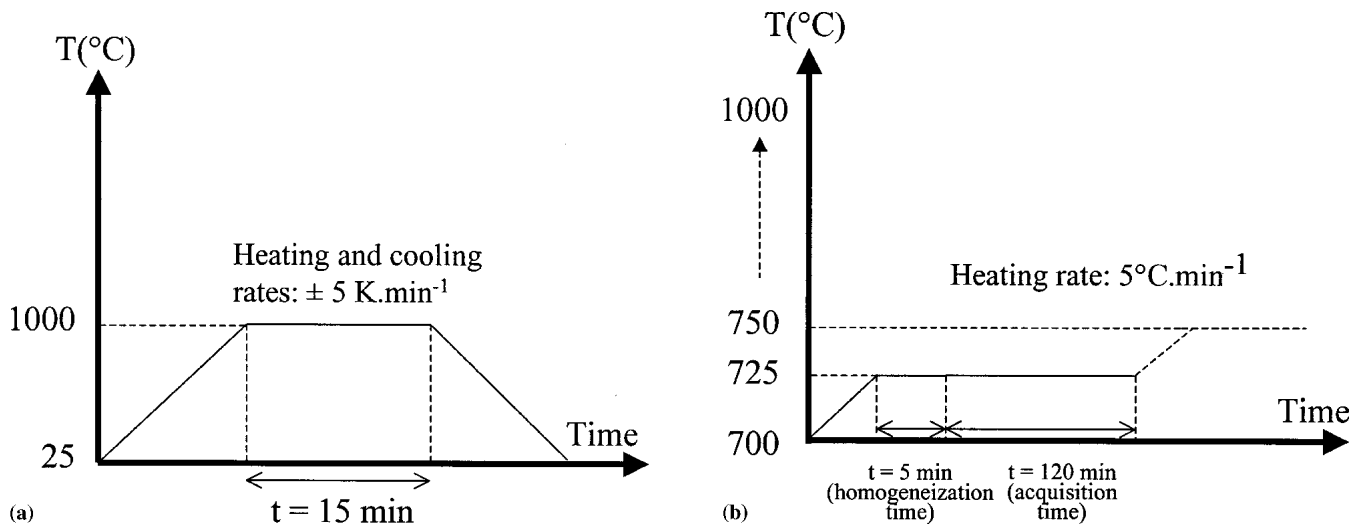


Fig. 3 Temperature programs used during (a) DSC and (b) HTXRD experiments.

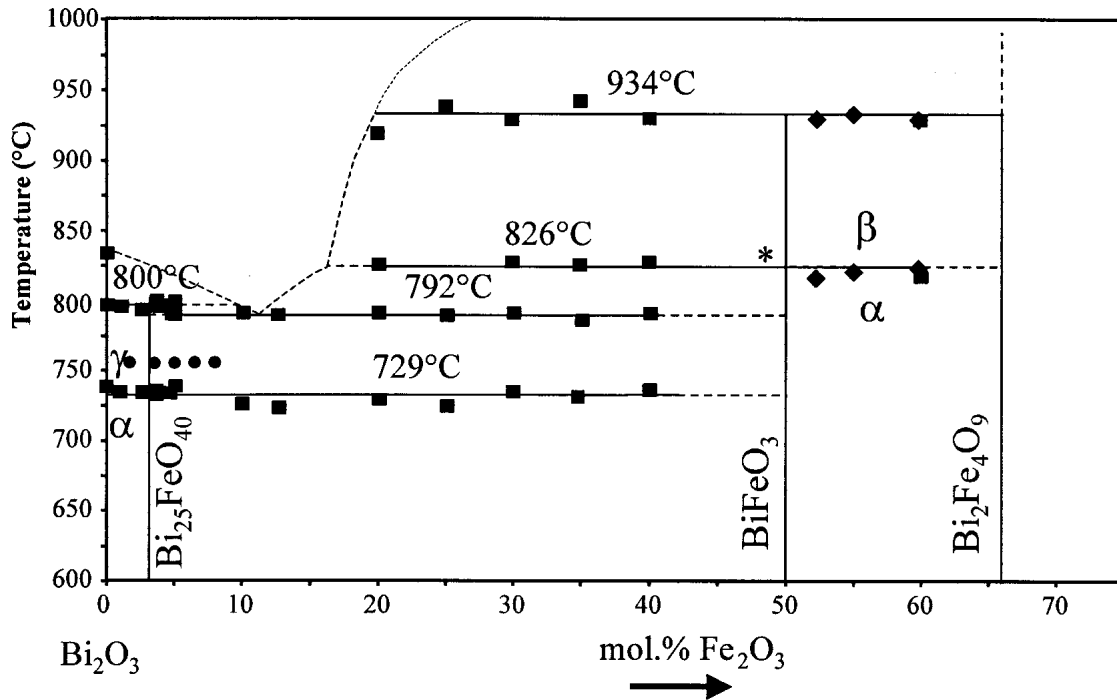


Fig. 4 Phase diagram $\text{Bi}_2\text{O}_3\text{-Fe}_2\text{O}_3$ in the temperature range 600-1000 °C. Equilibria (●) were characterized after long annealings. Invariant temperatures (■) were determined by DSC runs. Allotropic transitions (◆) were studied by HTXRD and DSC. The DSC arrests near 729 °C on either side of $\text{Bi}_{25}\text{FeO}_{40}$ possibly represent an allotropic transition in that phase though x-ray patterns (see Fig. 9) at $T > 729$ °C and $T < 729$ °C imply that the structural change is not major. Alternatively, these arrests may mean that the DSC samples in the composition range between $\text{Bi}_{25}\text{FeO}_{40}$ and BiFeO_3 retained some unreacted Bi_2O_3 . This hypothesis seems also to be ruled out by our EPMA studies. Detection thresholds were such that the results did not give theoretically any possibility of mistaking one phase for another. It is necessary to perform new experiments to decide definitively on this point. (*): It is impossible, given the uncertainty of the temperature measurements, to characterize any temperature difference between the two invariants on the left and the right of BiFeO_3 .

for several days at temperatures between 800 and 900 °C and quenched in ice gave the equilibrium concentrations. Furthermore, the morphology of the samples was also examined by optical microscopy (Olympus VANOX AHMT, Hamburg, Germany).

The polymorphic transformations in BiFeO_3 and $\text{Bi}_2\text{Fe}_4\text{O}_9$ were checked by x-ray diffraction at high temperatures. The scans were carried out with a Philips X'Pert Pro diffractometer (Eindhoven, The Netherlands) in the Bragg Brentano θ - 2θ geometry. A high-temperature cell

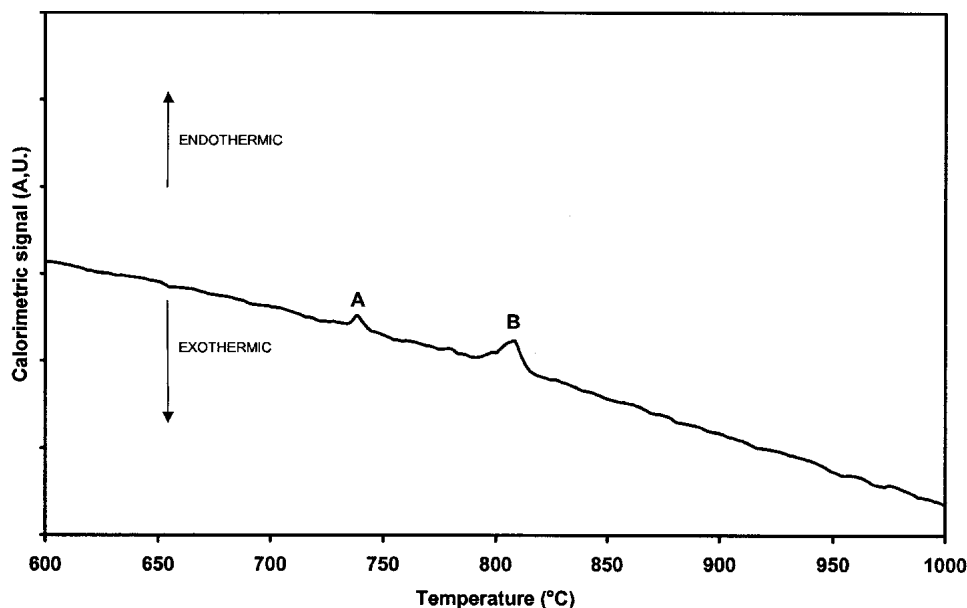


Fig. 5 DSC recording of the heating at 2 K min^{-1} of a sample with 1.3 mol.% Fe_2O_3

HTK 1200 from Anton Parr (Graz, Austria) was used and was equipped with a Kanthal APM furnace (Sandriken, Sweden), copper radiation ($\lambda_{\text{K}\alpha(\text{Cu})} = 0.14056 \text{ nm}$), kapton windows, and a rotating sample holder (30 rpm). This device is capable of working under vacuum or imposed atmosphere up to $1200 \text{ }^\circ\text{C}$. For BiFeO_3 , each pattern was recorded between 20 and 70° (2θ) with steps of 0.02° and 1.5 s counting time. Figure 3(b) gives schematically one step of the temperature program. To identify the phases, the search routine of the Diffract-AT software (Socabim, Paris, France) [1994Nus] was used. Moreover, the phases such as $\alpha\text{-BiFeO}_3$, $\beta\text{-BiFeO}_3$, and $\text{Bi}_{25}\text{FeO}_{40}$ were indexed from the JCPDS files 71-2494 [1971Mor], 72-2112 [1960Zas], and 46-0416 [1990Rad], respectively. To study the allotropic transformation in BiFeO_3 , the patterns recorded at 800 and $825 \text{ }^\circ\text{C}$ are analyzed by the Rietveld method with use of the program FULLPROF (Laboratoire Leon Brillouin, Saclay, France) [2000Rod]. The starting parameters were taken from [1969Mor] for the refinement of the low-temperature crystallographic structure ($800 \text{ }^\circ\text{C}$) and from [1969Tut] for the high-temperature structure ($825 \text{ }^\circ\text{C}$). Interatomic distances were calculated by using the IVTON software (Bioson Research Institute, Groningen, The Netherlands) [1988Vic].

3. Results and Discussion

The $\text{Bi}_2\text{O}_3\text{-Fe}_2\text{O}_3$ phase diagram was determined with the results from around twenty-five samples whose compositions were chosen between 0 and $75 \text{ mol.}\%$ Fe_2O_3 . Figure 4 presents the interpretation of all the experimental results.

3.1 Phase Limits and Invariants

On the Bi_2O_3 side of the system, no traces of iron in the phase Bi_2O_3 were detected, which means that the solubility

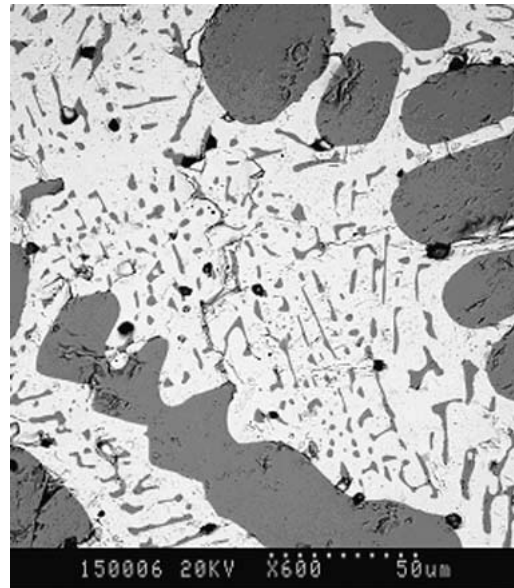
of Fe_2O_3 is probably lower than the detection threshold of the EPMA. As a consequence, the shape and size of the $\alpha + \gamma$ domain was out of reach. DSC experiments did not give any clear indications of either liquidus shape or composition. Reaction between the liquid products and the platinum crucible is a probable cause of this fact.

Figure 5 shows the DSC record obtained by heating sample with a $1.3 \text{ mol.}\%$ Fe_2O_3 . Two endothermic peaks (A and B) exist at 739 and $798 \text{ }^\circ\text{C}$, respectively. Above the temperature T_B , crossing the liquidus does not give any appreciable signal. It must be noted that

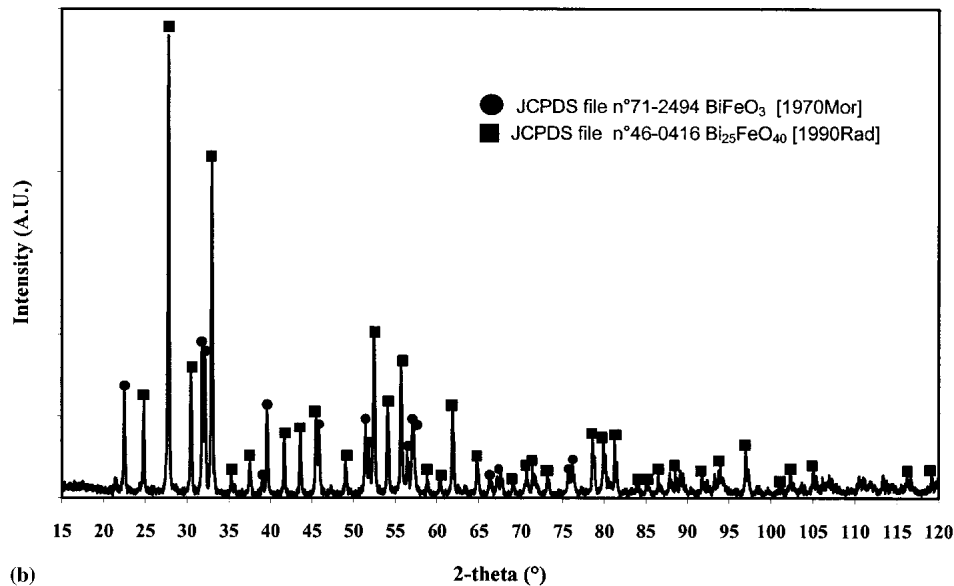
- The peak A corresponds to the polymorphic transformation in Bi_2O_3 : $\alpha \leftrightarrow \gamma$
- The peak B can be attributed to the peritectic:
 $\text{Bi}_2\text{O}_3 + \text{liq.} \leftrightarrow \text{Bi}_{25}\text{FeO}_{40}$

$\text{Bi}_{25}\text{FeO}_{40}$ is a stoichiometric phase that was detected during the course of this work. Speranskaya et al. [1965Spe] had already suspected a compound close to Bi_2O_3 , but they failed to accurately determine its chemical composition. A microprobe observation of a sample with $12.5 \text{ mol.}\%$ (Fig. 6a), after slow cooling (-2 K min^{-1}), shows the presence of two phases: $\text{Bi}_{25}\text{FeO}_{40}$ and BiFeO_3 . XRD on the same sample (Fig. 6b) confirmed the two compounds, with the majority being $\text{Bi}_{25}\text{FeO}_{40}$, which is cubic [1990Rad]. The stoichiometric designation as $\text{Bi}_{25}\text{FeO}_{40}$ is based on the analysis of the gray phase in Table 2.

Using all the experimental results, the invariant equilibria have been determined and compared with what was available in literature (Table 3). Obviously, the earlier results of Speranskaya et al. [1965Spe] are close to ours, the transformation temperatures found by these authors differ by less than $10 \text{ }^\circ\text{C}$ from those determined in this work.



(a)



(b)

Fig. 6 (a) SEM micrograph of the sample $0.125 \text{ mol} \cdot (\text{Bi}_2\text{O}_3) - 0.875 \text{ mol} \cdot (\text{Fe}_2\text{O}_3)$, heat-treated in the calorimeter up to 1000°C , then slowly cooled, and (b) XRD pattern at room temperature of the same product. The two phases are distinguished: BiFeO_3 gray and $\text{Bi}_{25}\text{FeO}_{40}$ light gray. Chemical analyses are given in Table 2.

3.2 Allotropic Transformations

Allotropic transformations were studied by high-temperature x-ray diffraction (HTXRD) for both $\text{Bi}_{25}\text{FeO}_{40}$ and BiFeO_3 . These experiments allowed us to check the temperatures already determined by DSC runs, but the values given by HTXRD are considered as only indicative due to the difficulty to ascertain the surface temperature of the sample.

3.2.1 BiFeO_3 phase. Figure 7 shows the results of HTXRD tests between 725 and 1000°C for a sample with $60 \text{ mol}\% \text{ Fe}_2\text{O}_3$. Between 800 and 825°C , a split of some lines of BiFeO_3 denotes a crystallographic transition. The

Table 2 Electron Probe Microanalysis Results of the Mixture $0.125 \text{ mol} \cdot (\text{Bi}_2\text{O}_3) - 0.875 \text{ mol} \cdot (\text{Fe}_2\text{O}_3)$ Shown in Fig. 6

Element	Bi	Fe	O
Detection threshold, at. %	0.14	0.21	0.25
Gray phase, at. %	19.87	19.81	60.32
Light gray phase, at. %	37.16	1.51	61.33

temperature detected by DSC (824°C) is in accordance with the HTXRD measurements. Figure 8 shows the Rietveld analyses at 800 and 825°C and the corresponding structural

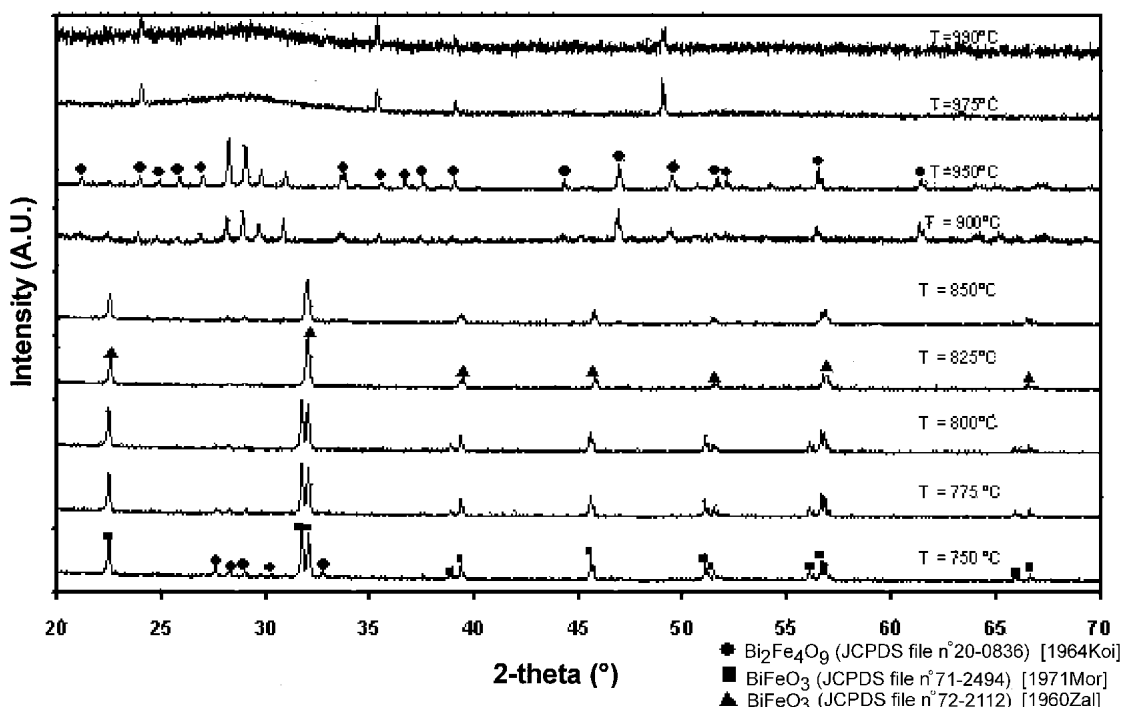


Fig. 7 High-temperature XRD patterns of a sample with 0.6 mol. Fe_2O_3 . The temperature program, which has been followed, is schematically illustrated in Fig. 3(b). It has not been noted that temperatures given are only indicative and less accurate than those given by DSC.

Table 3 Characteristics of the Main Invariant in the System Bi_2O_3 - Fe_2O_3 , This Work and Literature Data

Composition, Molar% Fe_2O_3	Temperatures, °C, Observed by DSC, Heating Rate, 2 K min ⁻¹											
	$\text{Bi}_{25}\text{FeO}_{40} + \text{BiFeO}_3 \leftrightarrow \text{Liq}$			$\text{Bi}_{25}\text{FeO}_{40} \leftrightarrow \text{Liq} + \text{Bi}_2\text{O}_3$			$\text{BiFeO}_3(\alpha) \leftrightarrow \text{BiFeO}_3(\beta)$			$\text{BiFeO}_3(\beta) \leftrightarrow \text{Liq} + \text{Bi}_2\text{Fe}_4\text{O}_9$		
	This Work	[1964 Koi]	[1965 Spe]	This Work	[1964 Koi]	[1965 Spe]	This Work	[1964 Koi]	[1965 Spe]	This Work	[1964 Koi]	[1965 Spe]
0.000	800	...	795
0.050	791	798	...	795
0.100	792	750	785
0.125	792	750	785
0.200	792	750	785	826	885	825	919	920	930
0.250	790	750	785	826	885	825	939	920	930
0.300	792	750	785	828	885	825	928	920	930
0.350	787	750	826	885	825	942	920	930
0.400	792	750	828	885	825	930	920	930
0.600	885	825	928	920	930

model with the FeO_6 octahedra representation. Below 824 °C, α - BiFeO_3 may be described as rhombohedral ($R3c$) with cell parameters, which were refined:

At 800 °C, $a = b = 0.5694(2)$ nm, and $c = 0.6885(2)$ nm.

Above 824 °C, β - BiFeO_3 is rhombohedral ($R3m$), and its cell parameters are

At 825 °C, $a = b = 0.56314(2)$ nm, and
 $c = 1.39850(7)$ nm.

This variety may also be described as a nearly ideal perovskite structure (cell angles $\alpha = \beta = \gamma \approx 90^\circ$). In addition, atoms positions are specified: Bi and Fe are on $1a$ positions while O is on $3b$. Atomic positions and distances are given in Table 4 and 5.

From a crystallographic point of view, the $\alpha \leftrightarrow \beta$ allotropic transition corresponds to:

- A lifting of degenerescency for the Fe-O distances. In the β high temperature form, Fe octahedral surrounding is defined by 6 equivalent Fe-O distances of 0.1992(1)

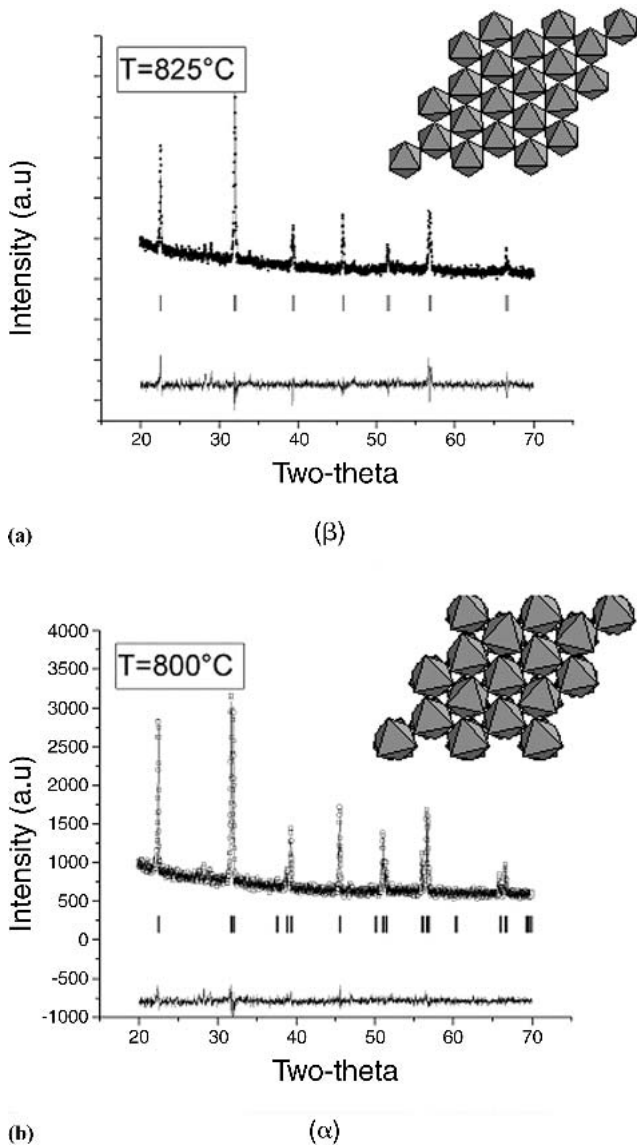


Fig. 8 Experimental (points) and computed (line) x-ray diffraction patterns for high (β) and low (α) temperature forms of BiFeO_3

nm. On the contrary, the α low temperature form is characterized by two different Fe-O distances of 0.197(5) and 0.218(5) nm, respectively.

- Rotations of the FeO_6 octahedra around the ternary axis (00z) leading to a superstructure of order two along this axis (Fig. 8a and 8b).

Above 900 °C, β - BiFeO_3 disappears to give $\text{Bi}_2\text{Fe}_4\text{O}_9$ and an amorphous (liquid) phase. Then, $\text{Bi}_2\text{Fe}_4\text{O}_9$ disappears above 975 °C.

3.2.2 $\text{Bi}_{25}\text{FeO}_{40}$ phase. A similar procedure was followed for several mixtures with different compositions in the two phase field $\text{Bi}_{25}\text{FeO}_{40}$ - BiFeO_3 . Results are presented for a 30 mol.% Fe_2O_3 mixture (Fig. 9), which gave the more clear patterns. BiFeO_3 lines are still of relative low intensities but at the same time give reference points.

Table 4 Interatomic Distances, nm, in BiFeO_3 for the Low Temperature (α , 800 °C) and the High-Temperature (β , 825 °C) Structures

Atom-Atom	<i>d</i> , nm, at 800 °C	<i>d</i> , nm, at 825 °C
Fe-O	6×0.1992 (1)	3×0.197 (5)
		3×0.218 (5)
		3×0.225 (6)
Bi-O	6×0.2814 (1)	3×0.250 (5)
	6×0.2820 (1)	3×0.332 (6)
		3×0.353 (6)
		3×0.348 (5)
Bi-Fe	2×0.3443 (1)	1×0.313 (2)
	6×0.3452 (1)	3×0.3594 (9)
		1×0.386 (2)

Table 5 Structural Parameters of BiFeO_3 for the Low-Temperature (α , 800 °C) and the High-Temperature (β , 825 °C) Structures

Parameter	At 800 °C, <i>R3c</i>	At 825 °C, <i>R3m</i>
a_h , nm	0.56314 (2)	0.5639 (1)
c_h , nm	1.3985 (1)	0.6886 (2)
a_r , nm		0.3984 (1)
α_r , °		90.11 (5)
Iron	In site (6a)	In site (3b)
<i>z</i> , Fe	0.224 (2)	0
Oxygen	In site (18b)	In site (9e)
<i>x</i> (O)	0.44 (1)	0.5
<i>y</i> (O)	0.023 (8)	0
<i>z</i> (O)	0.949 (4)	0
Bismuth	In site (6a) fixed at <i>z</i> = 0	In site (3a)

HTXRD patterns in the range 620-760 °C do not show any noticeable crystallographic modification, specially for $\text{Bi}_{25}\text{FeO}_{40}$ (Fig. 9). The face-centered-cubic (fcc) cell parameter of $\text{Bi}_{25}\text{FeO}_{40}$ changes from 1.0294(2) nm at 620 °C to 1.0318(3) nm at 760 °C, which is only due to thermal expansion. Consequently, from these results, it is not possible to confirm a crystallographic transition already suspected by DSC for $\text{Bi}_{25}\text{FeO}_{40}$. If a lattice parameter distortion occurs due to lowering of the symmetry, it might be of very small amplitude. In this case, the XRD pattern with the high resolution given by synchrotron radiation is necessary for determining the structural changes.

4. Conclusion and Future Work

The overall shape of the phase diagram deduced from this work is close to the one already proposed by Speranskaya et al. [1965Spe], but some points that were uncertain are now firmly established:

- The presence and chemical composition of $\text{Bi}_{25}\text{FeO}_{40}$ in the quasi binary system Bi_2O_3 - Fe_2O_3 were deter-

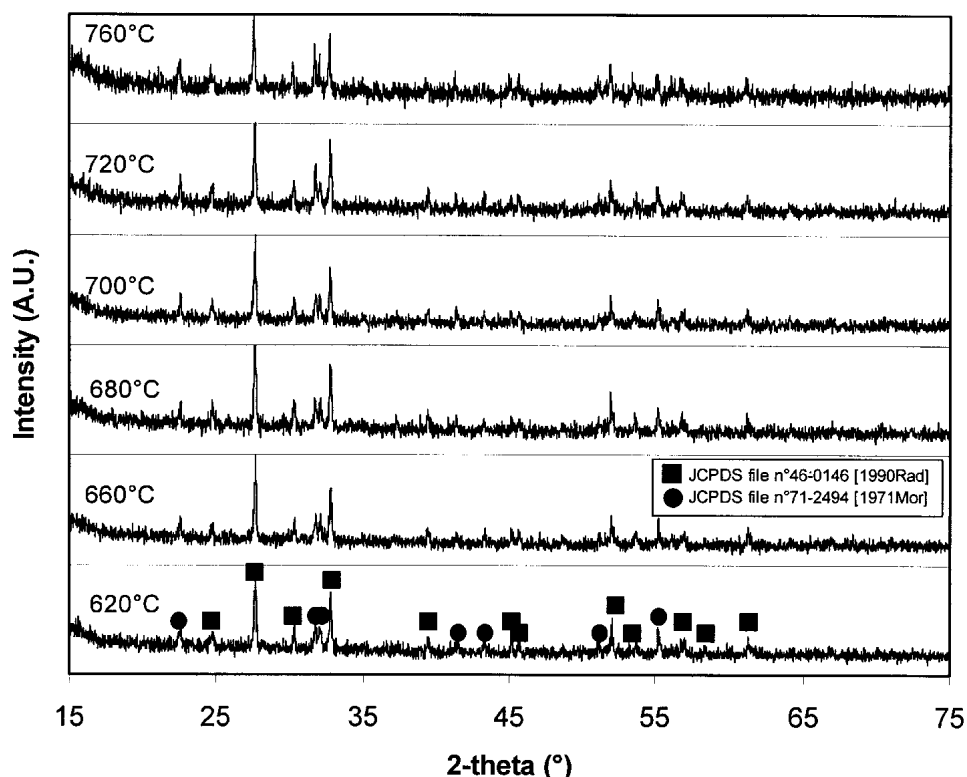


Fig. 9 XRD patterns between 620 and 760 °C for the composition like 0.3 mol.% Fe₂O₃ [with (■) for Bi₂₅FeO₄₀ and (●) for BiFeO₃]

mined by HTXRD and EPMA, which contradicts [1964Koi] and corrects [1965Spe].

- Eutectic and peritectic invariant temperatures were defined more accurately than before. The differences found between this work and those of [1964Koi] and [1965Spe] may be due to product purity and the sensitivity of the calorimeter which was used, not a differential thermal analysis device but a truly quantitative calorimeter [1986Gac].
- BiFeO₃ α ↔ β allotropic transition was established and structurally characterized.
- Bi₂₅FeO₄₀ was isolated.

There are still some points that need clarification:

- The liquidus shape is still unknown. The DSC experiments did not give indications about it, and its worth mentioning that the higher the temperature, the higher the uncertainty. The products, when above 1000 °C for a long time, attack the platinum crucible, and experiments become meaningless just before they destroy the calorimeter. A CALPHAD optimization may help on this point.
- An allotropic transition in Bi₂₅FeO₄₀ may exist.
- Oxygen pressure effects on the system have not yet been investigated.

Acknowledgments

This work was financially supported by the "Groupe de Recherche" (GDR) "GEDEON" involving CNRS,

EDF, and CEA. The authors are pleased to thank R. Podor and J.J. Kuntz for the technical help, especially during the calorimetry experiments, and J.P. Emeraux for the HTXRD studies.

References

- 1960Zas:** A.I. Zaslavsky and A.G. Tutov: "The Structure of a New Antiferromagnetic, BiFeO₃," *Dokl. Akad. Nauk*, 1960, 135, p. 815-17 (in Russian).
- 1964Koi:** H. Koizumi, N. Nirizaki, and T. Ikeda: "X-ray Study of the Bi₂O₃-Fe₂O₃ System," *Jpn. Appl. Phys.*, 1964, 3, pp. 495-96 (in Japanese).
- 1965Spe:** E.I. Speranskaya, V.M. Skorikov, E.Ya. Kode, and V.A. Terektova: "Phase Diagram of the System of Bismuth Oxide-Iron Oxide," *Bull. Acad. Sci. USSR*, 1965, 5, pp. 873-74 (in Russian).
- 1969Mor:** J.M. Moreau, C. Michel, R. Gerson, and W.J. James: "Ferroelectric BiFeO₃ X-ray and Neutron Diffraction Study," *Sol. State Commun.* 1969, 7, pp. 701-04.
- 1969Tut:** A.G. Tutov: "The Space Group and Some Electric and Magnetic Properties of Bismuth Ferrite," *Solid State Physics*, 1969, 11, pp. 2681-83.
- 1971Mor:** J.M. Moreau, C. Michel, R. Gerson, and W.J. James: "Ferroelectric Bismuth Ferrite BiFeO₃ X-ray and Neutron Diffraction Study," *J. Phys. Chem. Solids*, 1971, 32, pp. 1315-20.
- 1988Vic:** I. Vickovic: "CSU, A Highly Automatic and Selective Program for the Calculation and Presentation of Geometrical Parameters and Their e.s.d.s.," *J. Appl. Cryst.*, 1988, 21, pp. 987-90.
- 1986Gac:** J.C. Gachon: "Enthalpies of Formation of Transition Metal Binary Compounds by Direct Reaction in a 1800 K Calo-

- rimeter. Discussion of Thermodynamic and Structural Methods of Prediction,” Thesis d’Etat, University of Nancy, France, 1986 (in French).
- 1989Dim:** Y. Dimitriev, Ch. Petkov, E. Gattev, T. Stoilova and G. Gochev: “Study of the Structure of Bismuth Oxide-Iron Oxide ($\text{Bi}_2\text{O}_3\text{-Fe}_2\text{O}_3$) Glasses,” *J. Non-Cryst. Solids*, 1989, *112*, pp. 120-25.
- 1989Tan:** K. Tanaka, K. Kamiya, T. Yoko, S. Tanabe, K. Hirao, and N. Soga: “ESR and Mossbauer Studies of $\text{Bi}_2\text{O}_3\text{-Fe}_2\text{O}_3$ Glasses,” *J. Non-Cryst. Solids*, 1989, *109*, pp. 289-94.
- 1990Rad:** S. Radaev, L. Muradyan, and Yu. Kargin: “Neutron-Diffraction Study of the Sillenites Bismuth Iron Oxide ($\text{Bi}_{12}(\text{Bi}_{0.503}+\text{Fe}_{0.503})\text{O}_{19.50}$) and Bismuth Zinc Oxide ($\text{Bi}_{12}(\text{Bi}_{0.673}+\text{Zn}_{0.332})\text{O}_{19.33}$),” *Kristallografiya*, 1990, *35*, pp. 1126-30 (in Russian).
- 1994Iva:** S. Ivanov, S. Zhurov, and V. Karpov: *Kristallografiya*, 1990, *35*, pp. 1126 (in Russian).
- 1994Nus:** J. Nusovici and M.J. Winter: “Diffrac-AT Search, Search/Match Using Full Trace as Input,” *Adv. X-ray Anal.*, 1994, *37*, pp. 59-66.
- 1996Sos:** I. Sosnowska, R. Przenioslo, P. Fischer, and V.A.J. Murashov: “Neutron Diffraction Studies of the Crystal and Magnetic Structures of BiFeO_3 and $\text{Bi}_{0.93}\text{La}_{0.07}\text{FeO}_3$,” *J. Magn. Mater.*, 1996, *160*, pp. 384-85.
- 2000Kne:** J.U. Knebel, X. Cheng, C.H. Lefhalm, G. Muller, G. Schumacher, J. Konys, and H. Glasbrenner: “Design and Corrosion Study of a Closed Spallation Target Module of an Accelerator-Driven-System (ADS),” *Nucl. Eng. Design*, 2000, *202*, pp. 279-96.
- 2000Luo:** J. Luo and Y.M. Chiang: “Stabilization of Surface Films in Ceramics,” *Ceram. Trans.*, 2000, *118*, pp. 419-26.
- 2000Pas:** E.A. Pastukhov, S.A. Istomin, and N.V. Belousova: “Physico-Chemical Properties of $\text{Bi}_2\text{O}_3\text{-Fe}_2\text{O}_3$ and $\text{Bi}_2\text{O}_3\text{-V}_2\text{O}_5$ Melts,” *Inst. Metall., Rasplavy*, 2000, *1*, pp. 8-13.
- 2000Rod:** J. Rodriguez-Carvajal, *PROGRAM FullProf.2000 Multi-Pattern (Version 1.5)*, Laboratoire Léon Brillouin (CEA-CNRS), France (April 2000).
- 2001Bar:** F. Barbier and A. Rusanov: “Corrosion Behavior of Steels in Flowing Lead-Bismuth,” *J. Nucl. Mater.*, 2001, *296*, pp. 231-36.
- 2001Faz:** C. Fazio, G. Benamati, C. Martini, and G. Palombarini: “Compatibility Tests on Steels in Molten Lead and Lead-Bismuth,” *J. Nucl. Mater.*, 2001, *296*, pp. 243-48.
- 2002Mai1:** A. Maître, J.M. Fiorani, J.J. Kuntz, and J.C. Gachon, in *A Challenge in Metallurgy*, Proceedings of the Symposium Structural Materials for Hybrid Systems, “Preliminary Study of Some Parts of the Quinary System Bi-Fe-Hg-O-Pb.” D. Gorse and J.L. Boutard, ed., 2001, Paris, *J. Phys. IV*, 2002, *12*, pp. 163-74.
- 2002Mai2:** A. Maître, J.M. Fiorani, and M. Vilasi: “Thermodynamic Study of Phase Equilibria in the Pb-Bi-Hg System,” *J. Phase Equilibria*, 2002, *23*, pp. 329-38.
- 2002Vil:** C. Villagrasa, A. Boudard, J.C. David, L. Donadille, J.E. Ducruet, B. Fernandez, R. Legrain, S. Laray, C. Volant, W. Wlazlo, P. Ambrucstar, T. Engvist, F. Hammache, B. Jurado, K. Helariutta, K.H. Schmidt, K. Summarer, M.V. Ricciardi, F. Vives, C.O. Bacri, M. Barnas, B. Berthiet, L. Ferran, L. Audomin, B. Nustapha, F. Rajmund, C. Stephan, J. Taieb, L. Tassaut-Got, J. Benlliure, E. Casarujos, N. Fernandez, J. Pereira, S. Czajkowski, D. Karamanis, M. Prarikoff, J. George, R.A. Mewaldt, N. Yauasak, M. Niedenbeck, J. Connel, T. Faestermann, A. Heinz, and A. Junghans: “Residual Nuclei Produced by Spallation Reactions” in *A Challenge in Metallurgy*, Proceedings of the Symposium Structural Materials for Hybrid Systems, D. Gorse and J.L. Boutard, ed., 2001, Paris, *J. Phys. IV*, 2002, *12*, pp. 63-73.